AIP | Applied Physics Letters

Influence of Mn dopants on InAs/GaAs quantum dot electronic states

V. D. Dasika, A. V. Semichaevsky, J. P. Petropoulos, J. C. Dibbern, A. M. Dangelewicz et al.

Citation: Appl. Phys. Lett. **98**, 141907 (2011); doi: 10.1063/1.3567510
View online: http://dx.doi.org/10.1063/1.3567510
View Table of Contents: http://apl.aip.org/resource/1/APPLAB/v98/i14
Published by the AIP Publishing LLC.

Influence of Mn dopants on InAs/GaAs quantum dot electronic states

V. D. Dasika,[1,2] A. V. Semichaevsky,[3] J. P. Petropoulos,[4] J. C. Dibbern,[2] A. M. Dangelewicz,[2] M. Holub,[1] P. K. Bhattacharya,[1] J. M. O. Zide,[4] H. T. Johnson,[3] and R. S. Goldman[1,2,a)]

[1]*Department of Electrical Engineering and Computer Science, University of Michigan, Ann Arbor, Michigan 48109-2122, USA*

[2]*Department of Materials Science and Engineering, University of Michigan, Ann Arbor, Michigan 48109-2136, USA*

[3]*Department of Mechanical Science and Engineering, University of Illinois at Urbana-Champaign, Urbana, Illinois 61801, USA*

[4]*Department of Materials Science and Engineering, University of Delaware, Newark, Delaware 19716, USA*

(Received 1 November 2010; accepted 16 February 2011; published online 6 April 2011)

We have investigated the influence of Mn dopants on the electronic states in the vicinity of InAs/GaAs quantum dots (QDs) and the surrounding GaAs matrix. A comparison of cross-sectional scanning tunneling microscopy, scanning tunneling spectroscopy, and tight binding calculations of the local density of states reveals that the Mn dopants primarily influence the electronic states at the QD edges and the surrounding GaAs matrix. These results suggest that the Mn dopants reside at the QD edge, consistent with the predictions of a thermodynamic model for the nanoscale-size dependence of dopant incorporation in nanostructures. © *2011 American Institute of Physics*. [doi:10.1063/1.3567510]

Doping of III-V semiconductors with transition metals such as manganese (Mn) leads to simultaneous semiconducting and ferromagnetic behavior, thus enabling devices such as spin-valves and spin-injection contacts.[1–4] In the case of quantum dot (QD) structures, Mn-doping enables the achievement of spin-polarized optoelectronic devices such as lasers and light emitting diodes.[3,4] For epitaxially grown GaMnAs heterostructures, ferromagnetism has been reported below the Curie temperature of ~180 K, although ion beam-induced MnAs nanoclusters in GaAs have led to Curie temperatures as high as 360 K.[5,6] Furthermore, for InAs:Mn QDs, Curie temperatures >300 K have been reported.[3,7] However, there have been conflicting reports on the distribution of the Mn dopants in the InAs:Mn QDs and surrounding matrix. One group reported transmission electron microscopy-based electron energy loss spectroscopy measurements of large (36 ± 1 nm diameter) InAs:Mn QDs, suggesting that Mn dopants reside primarily in the QD core.[7] Another group showed cross-sectional scanning tunneling microscopy (XSTM) evidence of significant Mn surface segregation during InAs:Mn QD growth, and suggested that the majority of the Mn dopants in small (<20 nm diameter) QDs are located at the edges of the QD and/or in the GaAs matrix outside the QD.[8] In terms of electronic states, evidence for mid-gap states has been observed in scanning tunneling spectroscopy (STS) spectra of bulklike GaAs:Mn (Ref. 9) and InAs:Mn.[10] To date, the influence of Mn dopants on the electronic states of InAs:Mn QDs has not been reported.

Here, we report an analysis of the atomic-scale distribution of Mn dopants and its influence on the electronic states of InAs:Mn QDs and the surrounding GaAs matrix, using XSTM (Ref. 11) and STS,[12] in comparison with order(N) tight-binding calculations of the local density of states (LDOS).[13] This approach allows us to deduce the positions of the dopants based on their influence on the LDOS. STS spectra from various locations in InAs and InAs:Mn QDs were compared with the LDOS of InAs and InAs:Mn QDs, calculated with Mn at the QD core, QD edge, or in the GaAs matrix. The observed trends in LDOS match those of the measured STS spectra only for the case of Mn at the QD edge, and not for the cases of Mn at the QD core or in the GaAs matrix. Together, these results suggest that the Mn dopants preferentially reside near the edges of the QD, consistent with the predictions of a thermodynamic model for the nanoscale-size dependence of dopant incorporation in nanostructures.

For these studies, heterostructures consisting of InAs:Be QDs and InAs:Mn QDs, separated by 20 nm of GaAs, were grown on (001)-oriented *p*+ GaAs; undoped InAs QD heterostructures were grown separately.[7,12] For XSTM, the samples were cleaved to expose a $(1\bar{1}0)$ surface, in an ultrahigh vacuum chamber with base pressure $<5 \times 10^{-11}$ Torr. To measure the differential conductance of individual QDs and the surrounding GaAs matrix, we used STS with the variable tip-sample separation method. To calculate the LDOS of the In and Ga atoms, we used a moments-based order(N) tight-binding approach.[13] We accounted for the effects of Mn impurities on the LDOS through their $s-d$ and $p-d$ exchange interactions with the host anions, and their Coulomb interaction energies. Additional details of the sample growth, STS measurement and analysis, and tight-binding calculations are provided in Ref. 14.

Figure 1 shows an example of a large-scale XSTM image of the InAs:Be and InAs:Mn QDs. The bright regions toward the top (bottom) of the image correspond to the InAs:Mn (InAs:Be) QDs. Monolayer height steps are also visible toward the top of Fig. 1. The typical QD diameters are 12 ± 2 nm and typical QD heights are 4 ± 1 nm. The average lateral spacing between the QDs is 87 ± 30 nm.

a)Author to whom correspondence should be addressed. Electronic mail: rsgold@umich.edu.

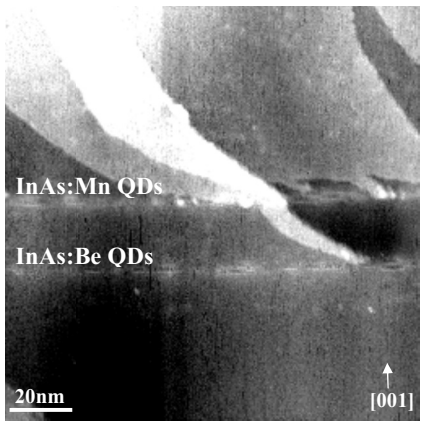

FIG. 1. Large-scale XSTM topographic image acquired with a constant tunneling current of 0.5 nA and a sample bias of −2.0 V. The bright regions toward the top (bottom) of the image correspond to the InAs:Mn (InAs:Be) QDs. The gray-scale range displayed is 0.7 nm.

Figure 2 presents STS spectra collected from the (a) QD core, (b) QD edge, and (c) GaAs matrix to compare the InAs, the InAs:Be, and the InAs:Mn QDs. For each spectrum, the effective valence (E_V) and conduction (E_C) band edges are indicated by vertical dashed lines at negative and positive sample voltages, respectively. The top, center, and bottom plots show the measured normalized conductance from the InAs:Mn, InAs:Be, and InAs QDs respectively. For GaAs, the measured bandgap is slightly larger than the predicted 1.42 eV, likely due to tip-induced band bending. The effective bandgaps of the QDs are lower than those of GaAs, consistent with trends reported in the literature.[12,15–18]

In Figs. 2(a) and 2(b), spectra from the core and edge of the InAs QDs show well-defined effective band edges, without electronic states within the bandgap. In addition, the effective bandgap decreases laterally toward the QD core, presumably due to variations in [In], consistent with previous reports.[12,17–19] At the core of the InAs:Mn QDs, shown in Fig. 2(a), the STS spectra are similar to those of the InAs QDs, with well-defined band edges and negligible electronic states within the bandgap. Near the edge of the InAs:Mn QDs, several additional spectral features, indicated by arrows in Fig. 2(b), are observed in the vicinity of E_C and E_V, most likely due to states associated with Mn. Thus, the electronic structure of the doped InAs:Mn QDs is altered most significantly near the QD edges, suggesting that the Mn dopants preferentially reside near the edges of the QD. This is further supported by the STS spectra from the GaAs matrix in the immediate vicinity of the QDs, shown in Fig. 2(c), which reveal well-defined band edges, without mid-gap spectral features. However, for the GaAs matrix in the immediate vicinity of the InAs:Mn QDs, several mid-gap features are observed. Similar trends were also observed for the InAs:Be QDs, as shown in Fig. 2.

For comparison, as shown in Fig. 3, we consider the LDOS calculated at the QD edge, QD core, and surrounding GaAs matrix, with and without Mn dopants at each location. The LDOS calculations reveal InAs and InAs:Mn QD effective bandgaps that are lower than those of the surrounding GaAs matrix, consistent with the data discussed above. As shown in Figs. 3(a)–3(c), the LDOS calculated at the QD core (13 lattice spacings from the edge) exhibit negligible electronic states within the gap. Thus, the QD core LDOS is predicted to be insensitive to the presence of Mn dopants,

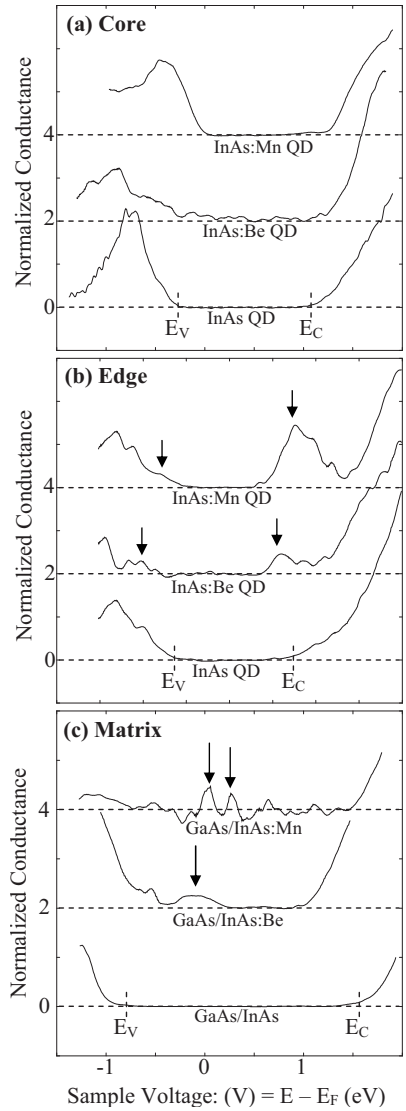

FIG. 2. Plot of normalized conductance versus sample bias, collected from the (a) core, (b) edge, and (c) GaAs matrix surrounding InAs, InAs:Be, and InAs:Mn QDs. The sample voltage corresponds to the energy relative to the Fermi level. The effective valence (E_V) and conduction (E_C) band edges are indicated by vertical dashed lines at negative and positive sample voltages, respectively. The spectra from the QD core are similar for all cases. In the spectra from the edge of the InAs:Mn QDs and from the GaAs near the edges of InAs:Mn QDs, mid-gap features indicated by vertical arrows presumably correspond to Mn-induced electronic states.

independent of the location of the Mn dopant within the QD or matrix.

For the cases of the LDOS calculated two lattice spacings from the QD edge [Figs. 3(d)–3(f)] and in the surrounding GaAs matrix [Figs. 3(g)–3(i)], when the Mn dopants are assumed to be located at the QD core, negligible midgap spectral features are apparent in the LDOS, as shown in Figs. 3(d) and 3(g). However, when the Mn dopants are assumed to be located near the QD edge or in the surrounding GaAs matrix, additional spectral features are apparent in the LDOS, as indicated by arrows in Figs. 3(e), 3(f), and 3(h). Interestingly, for the "Mn at QD edge" case, the spectral features apparent in the LDOS calculated at the QD core [Fig. 3(b)], the QD edge [Fig. 3(e)], and in the surrounding GaAs matrix [Fig. 3(h)] are consistent with the STS data in Fig. 2. Thus, it is likely that the Mn dopants are preferentially located at the QD edges. Together, the STS data and

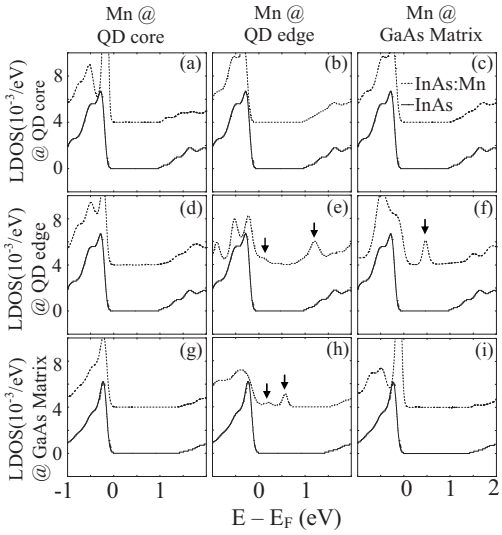

FIG. 3. The LDOS calculated at the QD core (a)–(c), QD edge (d)–(f), and GaAs matrix (g)–(i), using order (N) tight binding. LDOS from in and near the InAs:Mn (InAs) QDs are plotted as dashed (solid) lines toward the top (bottom). The LDOS was calculated assuming three different cases: Mn located at the QD core [(a), (d), and (g)], Mn located at the QD edge [(b), (e), and (h)], and Mn located in the surrounding GaAs matrix [(c), (f), and (i)]. The trends observed in the "Mn at QD edge" case are consistent with the trends observed in the measured STS spectra.

the calculated LDOS reveal that the Mn dopants within the QD influence the electronic structure of both the QD and the surrounding GaAs matrix.

This finding is in agreement with earlier studies of small, but not large, InAs:Mn QDs. We therefore consider the nanoscale-size dependence of Mn incorporation in InAs QDs. Using a thermodynamic model described elsewhere,[20] we assume a 2 to 80 nm diameter spherical InAs nanoparticle in a GaAs matrix. We calculate the Gibbs free energy assuming that Mn atoms at the QD core (surface) displace four In–As (three In–As and one Ga–As) bonds. We use literature values for the In–As and Ga–As bond energies,[21] and a Mn–As bond energy calculated using the reported bulk solubility of Mn in GaAs.[22] The resulting Mn-induced change in Gibbs free energy, ΔG, as a function of QD diameter, is shown in Fig. 4, where the solid (dashed) lines represent the cases of a Mn atom at the core (surface) of the InAs QD. When $\Delta G < 0$, Mn incorporation is predicted to occur. It is most energetically favorable for Mn to incorporate in the

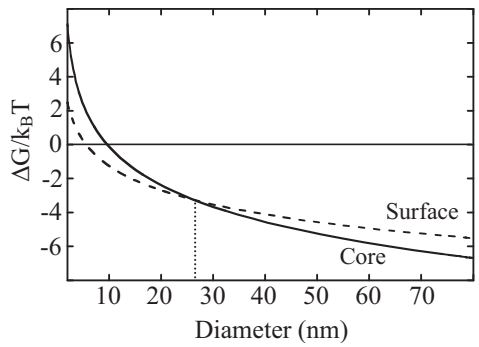

FIG. 4. Normalized Gibbs free energies for single Mn impurities, plotted as a function of InAs QD diameter. The solid and dashed curves represent the free energy for Mn impurities at the QD core and surface. Above (below) a critical QD diameter of 26 nm, core (surface) doping is expected to dominate.

configuration that has the lowest value of ΔG. Thus, for the largest QDs, Mn is predicted to incorporate at the core, consistent with Ref. 7. As the QD size is decreased to below 26 nm,[23] Mn prefers to incorporate at the edges, as we show here.

We gratefully acknowledge partial support of the U.S. Department of Energy, Office of Science, Office of Basic Energy Sciences under Grant No. DE-FG02-06EF46339. A.V.S., J.C.D., and A.M.D. were supported in part by the National Science Foundation through Grant No. CBET 09-33348. V.D.D. and R.S.G. were supported in part by the Center for Solar and Thermal Energy Conversion, an Energy Frontier Research Center funded by the U.S. Department of Energy, Office of Science, Office of Basic Energy Sciences under Award No. DE-SC0000957. J.P.P. and J.M.O.Z. were supported in part by the Office of Naval Research under Award No. N00014-09-1-0747.

[1]H. Ohno, D. Chiba, F. Matsukura, T. Omiya, E. Abe, T. Dietl, Y. Ohno, and K. Ohtani, Nature (London) **408**, 944 (2000).
[2]Y. Ohno, D. K. Young, B. Beschoten, F. Matsukura, H. Ohno, and D. D. Awschalom, Nature (London) **402**, 790 (1999).
[3]S. Chakrabarti, M. A. Holub, P. Bhattacharya, T. D. Mishima, M. B. Santos, M. B. Johnson, and D. A. Blom, Nano Lett. **5**, 209 (2005).
[4]M. Holub, J. Shin, S. Chakrabarti, and P. Bhattacharya, Appl. Phys. Lett. **87**, 091108 (2005).
[5]M. Wang, R. P. Campion, A. W. Rushforth, K. W. Edmonds, C. T. Foxon, and B. L. Gallagher, Appl. Phys. Lett. **93**, 132103 (2008).
[6]A. Serres, G. Benassayag, M. Respaud, C. Armand, J. C. Pesant, A. Mari, Z. Liliental-Weber, and A. Claverie, Mater. Sci. Eng., B **101**, 119 (2003).
[7]M. Holub, S. Chakrabarti, S. Fathpour, P. Bhattacharya, Y. Lei, and S. Ghosh, Appl. Phys. Lett. **85**, 973 (2004).
[8]M. Bozkurt, V. A. Grant, J. M. Ulloa, R. P. Campion, C. T. Foxon, E. Marega, G. J. Salamo, and P. M. Koenraad, Appl. Phys. Lett. **96**, 042108 (2010).
[9]D. Kitchen, A. Richardella, J.-M. Tang, M. E. Flatte, and A. Yazdani, Nature (London) **442**, 436 (2006).
[10]F. Marczinowski, J. Wiebe, J.-M. Tang, M. E. Flatte, F. Meier, M. Morgenstern, and R. Wiesendanger, Phys. Rev. Lett. **99**, 157202 (2007).
[11]J. N. Gleason, M. E. Hjelmstad, V. D. Dasika, R. S. Goldman, S. Fathpour, S. Charkrabarti, and P. K. Bhattacharya, Appl. Phys. Lett. **86**, 011911 (2005).
[12]V. D. Dasika, R. S. Goldman, J. D. Song, W. J. Choi, N. K. Cho, and J. I. Lee, J. Appl. Phys. **106**, 014315 (2009).
[13]A. D. Schuyler, G. S. Chirikjian, J.-Q. Lu, and H. T. Johnson, Phys. Rev. E **71**, 046701 (2005).
[14]See supplementary material at http://dx.doi.org/10.1063/1.3567510 for details on sample growth, STS measurement and analysis, and ONTB calculations.
[15]T. Yamauchi, Y. Matsuba, L. Bolotov, M. Tabuchi, and A. Nakamura, Appl. Phys. Lett. **77**, 4368 (2000).
[16]B. Legrand, B. Grandidier, J. P. Nys, D. Stievenard, J. M. Gerard, and V. Thierry-Mieg, Appl. Phys. Lett. **73**, 96 (1998).
[17]D. M. Bruls, J. W. A. M. Vugs, P. M. Koenraad, M. S. Skolnick, M. Hopkinson, and J. H. Wolter, Appl. Phys. A: Mater. Sci. Process. **72**, S205 (2001).
[18]S. Gaan, G. He, R. M. Feenstra, J. Walker, and E. Towe, Appl. Phys. Lett. **97**, 123110 (2010).
[19]J. Q. Lu, H. T. Johnson, V. D. Dasika, and R. S. Goldman, Appl. Phys. Lett. **88**, 053109 (2006).
[20]J. P. Petropoulos, T. R. Cristiani, P. B. Dongmo, and J. M. O. Zide, Nanotechnology (to be published).
[21]D. R. Lide, *CRC Handbook of Chemistry and Physics*, 90th ed. (CRC, Boca Raton, FL, 2010).
[22]H. Ohno, A. Shen, F. Matsukara, A. Oiwa, A. Endo, S. Katsumoto, and Y. Iye, Appl. Phys. Lett. **69**, 363 (1996).
[23]We note that the absolute value of ΔG is influenced by the value of the Mn–As bond energy but the core-shell crossover size indicated in Fig. 4 is largely unaffected.